March 4 2021

Measurement of Boltzmann's Constant Using Noise Characteristics of Resistors

Georgia Institute of Technology

Electronics II with Professor First

Robert Pierrard

INTRODUCTION

As one studies electronics they are bound to come across the implications of noise in their circuits. To conduct precise experimentation, one must develop skills to effectively control such noise. They must understand its sources, how it propagates through a circuit, and how to minimize its effects. The purpose of this lab is to develop an understanding of one of the most fundamental sources of noise, Johnson noise, as well as the voltage and current noise produced from active components such as op amps. To exemplify a strong understanding of the relevant noise concepts, this lab will culminate with calculating Boltzmann's constant by measuring the resistor noise output for various resistance values.

BACKGROUND

In completing this lab, the Texas Instruments Noise Analysis in Operational Amplifier Circuits Application Report, as well as several analog tutorials from Analog Devices, were followed as both learning tools and reference guides. Noise can be generated by countless sources such as a loud truck driving down the street near your experiment. However, in the application report, only five main noise sources were discussed. Further, only three of these five sources, Shot, Johnson, and Flicker noise, are relevant for this lab. The three succeeding definitions are sourced directly from the Texas Instruments Application Report.

Shot Noise - Shot noise is associated with current flow. Shot noise results whenever charges cross a potential barrier, like a PN junction. Crossing the potential barrier is a purely random event. Thus, the instantaneous current, i, is composed of a large number of random, independent current pulses with an average value, i_D. Shot noise is spectrally flat or has a uniform power density, meaning that when plotted versus frequency, it has a constant value. Shot noise is independent of temperature. The mean squared value of shot noise can be written as:

$$\overline{i_n^2} = \overline{(i - i_D)^2} = \int 2qi_D df$$

Where qi_D is a current power density having units of A^2/Hz.

Johnson Noise - Thermal noise is caused by the thermal agitation of charge carriers (electrons or holes) in a conductor. This noise is present in all passive resistive elements. Like shot noise, thermal noise is

spectrally flat or has a uniform power density, but thermal noise is independent of current flow. Thermal noise in a conductor can be modeled as voltage or current. When modeled as a voltage it is placed in series with an otherwise noiseless resistor. When modeled as a current it is placed in parallel with an otherwise noiseless resistor. The average mean-square value of the voltage noise source or current noise source is calculated by:

$$\overline{e^2} = \int 4kTRdf \text{ or } \overline{i^2} = \int (4kT / R)df$$

Where k is Boltzmann's constant, T is the absolute temperature in Kelvin, and R is the resistance of the conductor in Ohms.

Flicker Noise - Flicker noise is also called 1/f noise. It is present in all active devices and has various origins. Flicker noise is always associated with a dc current, and its average mean-square value is of the form:

$$\overline{e^2} = \int \left(K_e^2 / f\right) df \text{ or } \overline{i^2} = \int \left(K_i^2 / f\right) df$$

Where K_e and K_i are the appropriate device constants (in volts or amps).

PROCEDURES

This lab contains four natural divisions in which we can divide the procedure and results.

Section I - To begin this lab, we will compare the noise characteristics of three different op amps, the AD795, the LT1017, and the OP27. This is accomplished by following the procedure on page four of the Analog Devices tutorial MT-047. By changing the value of resistor R_1 we see different output values for noise spectrum of the circuit. With these data, and confirmation from the op amp specs, we can understand the dominant noise source from the op amp circuit three different input impedances (100, 100k, and 1Meg). Rather than physically constructing the circuit, it is reproduced in LTspice. To minimize input bias currents, $R_1 = R_2||R_3$ is maintained when changing resistance values. The circuit construction is shown below.

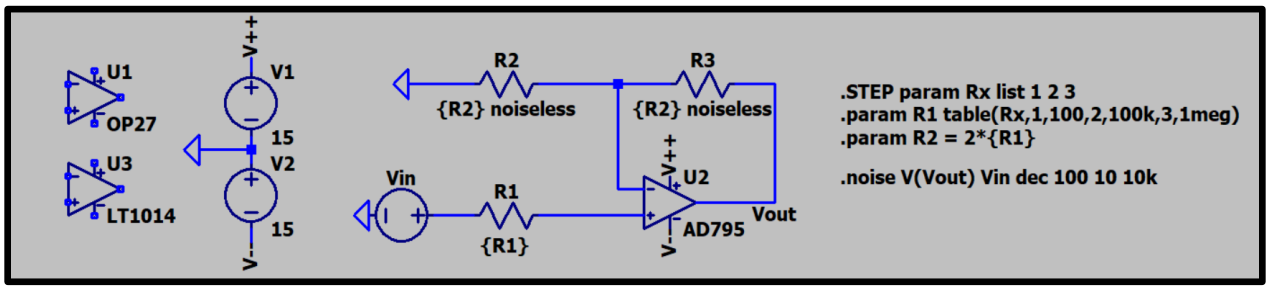

As opposed to the experiment conducted by Analog Devices, when measuring the output noise this simulation will display the noise spectrum for each individual op amp with three different resistor values.

Section II - For the second part of this lab, we will be construction a circuit which attempts to measure the Johnson noise of various resistors. After trying other configurations, the following instrumentational amplifier circuit was chosen.

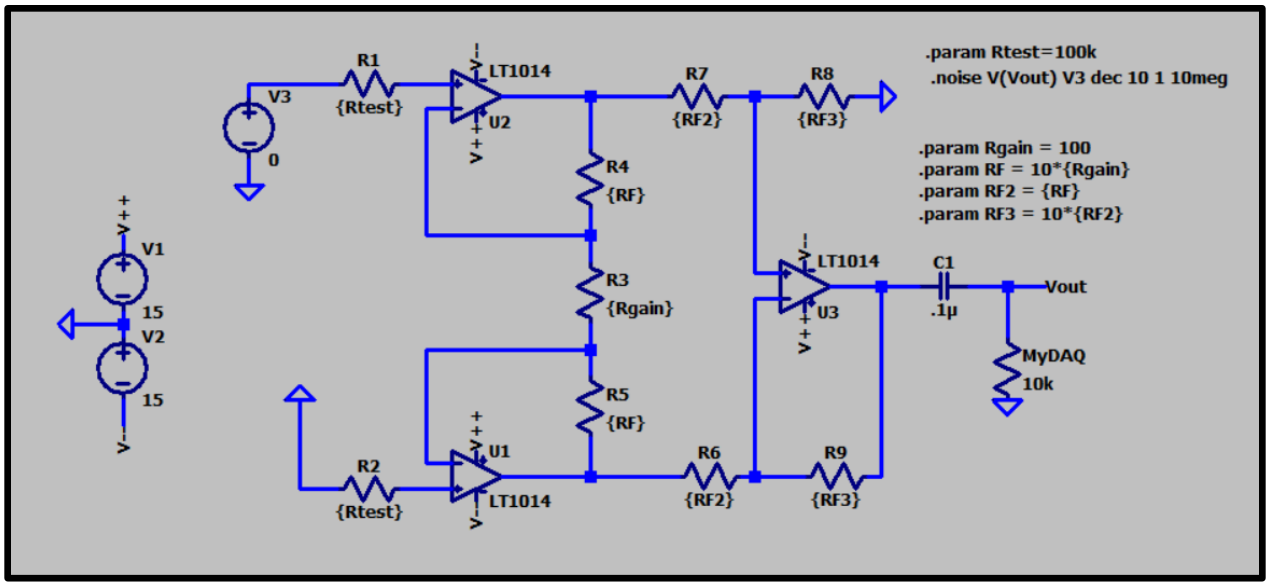

After constructing this circuit in LTspice and running the noise command, we can probe V_{out} to get the noise spectrum and peak noise density for the total noise of the circuit. Thanks to the power of simulation, we can probe the test resistor itself to see its contributions to the noise output. For both the total output noise and the contribution from the test resistor, we can also get the total RMS noise over the simulations specified frequency band (1Hz-10MHz). Data for both the frequency spectrum and RMS noise for the test resistor and the total output noise are stored in a spreadsheet and shown in Table 1 of Results section II.

Now following the aforementioned tutorial from Texas Instruments, we derive hand calculations for the total RMS noise at the output of the circuit. This procedure consists of treating each noise source independent from the rest and multiplying its contribution by its gain through the circuit. We hope our hand calculation is within a factor of 5 from the total RMS noise given by LTspice.

Section III - Now, we want to use LTspice to predict how the noise scales with R_{test}. Our hope is that for large enough R_{test}, Johnson noise from R_{test} becomes the largest source of noise.

For various values of R_{test}, ranging from 100Ω to 10MΩ, we will perform the noise simulation where we will record the peak spectral noise density and total RMS noise through R_{test} and at V_{out}. These data can be found in Table 1 of Results III.

By plotting the total RMS noise vs R_{test} we can estimate the value of $K_B T$ at room temperature. The exact calculation can be found in Results III.

Section IV – For the final part of this lab, we will repeat the procedure in Section III but with a physical circuit rather than a simulation. First, we must construct the circuit on the MyDAQ breadboard. An image of the circuit can be found below.

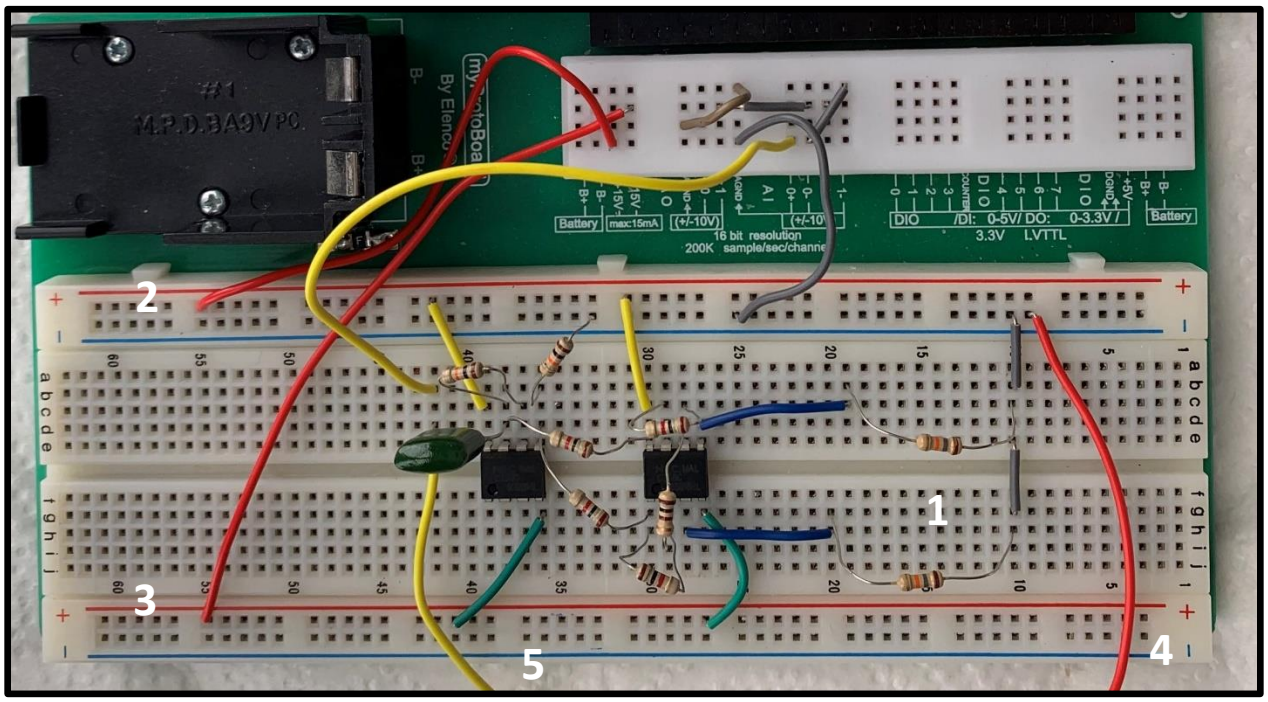

The inner workings of this circuit follow the schematic presented previously. There are, however, a few clarifications/distinctions that should be made. The enumeration of the following bullets corresponds to the numbers displayed in the image above.

1. The resistors above and below here are the test resistors. They are swapped with different resistors as the value for R_{test} changes but they are always identical and connected to ground.
2. This is the positive 15 Volt power rail.
3. This is the negative 15 Volt power rail.
4. This wire is used to ground the (not yet discussed) shielding around the circuit.
5. This wire is left floating outside of the shielding and will be used to ground the output of the circuit prior to measurement. The requirement for this wire will be discussed later.

Now, considering we are using this circuit to measure the Johnson noise through the test resistors, it is extremely sensitive to other sources of noise (such as nearby computers/monitors). For this reason, we must shield the circuit from its surroundings. This is achieved with a metal enclosure composed of an aluminum foil bottom surface with a baking pan as a lid. Wire 4 in the above picture is attached to the aluminum foil to ground the enclosure. Note that there are many exposed pins on the bottom of the MyDAQ breadboard, therefore the bottom of the breadboard must be separated from the aluminum foil to avoid unintentional grounding. Whenever measurements are being made, the baking pan should be put over top of the circuit, in full contact with the aluminum foil.

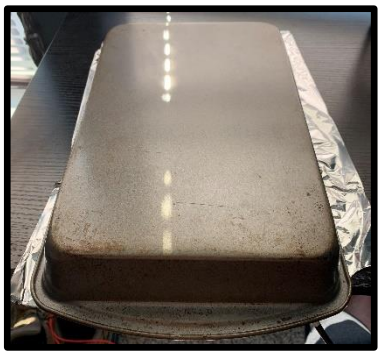

Once the circuit is constructed and shielded, the next task is to make our measurements. Using the MyDAQ Bode Analyzer measure and record the gain as a function of frequency for the circuit. With the high gain of the circuit explained above, it will be necessary to reduce the amplitude of the input. A well-behaved output is produced when the MyDAQ's minimum input value (10mV) is used.

Finally, for multiple values of R_{test} (up to 10MΩ), measure both the total RMS noise at the output of your circuit with the MyDAQ Oscilloscope. These measurements contain a large degree of variability. For more accurate data, take multiple measurements for each resistance and calculate the average. As done with the simulation data, use these values to calculate Boltzmann's constant and make comparisons between the simulation and the physical circuit.

Furthermore, when changing out resistors, a considerable offset voltage is produced at the output. Therefore, to "reset" the experiment after changing resistors, you must ground the output of the circuit. Furthermore, sometimes when the circuit is fully assembled the output voltage will slowly drift to higher and higher voltages. So, to collect accurate data, the output must be grounded before taking each measurement. The wire at 5 in the above image was added so that the circuit can be grounded with the shielding already in place. This grounding takes care of both output voltage drifting problems.

RESULTS

The data/results and corresponding calculations for each of the sections explained in the Procedure section are given below. These results are explained in the following Discussion section.

Section I – In the following three noise spectrums the R_{Test} values are as follows. Green = 100Ω, Blue = 100kΩ, Red = 1MΩ.

Figure 1: AD795 Noise Spectrum

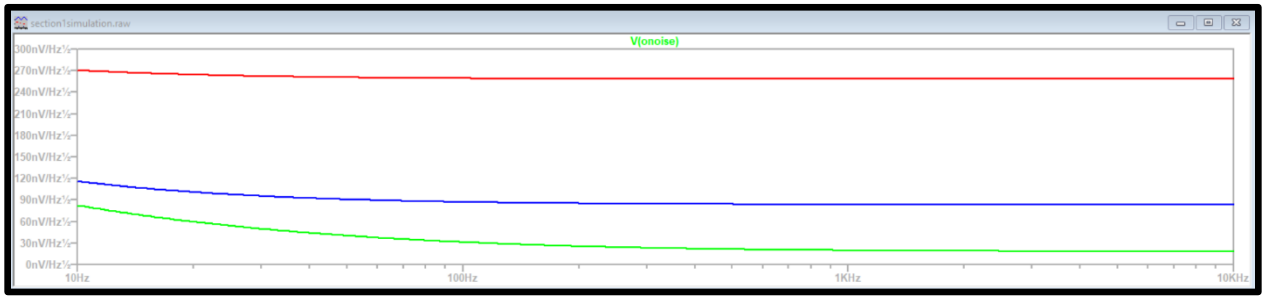

Figure 2: LT1014 Noise Spectrum

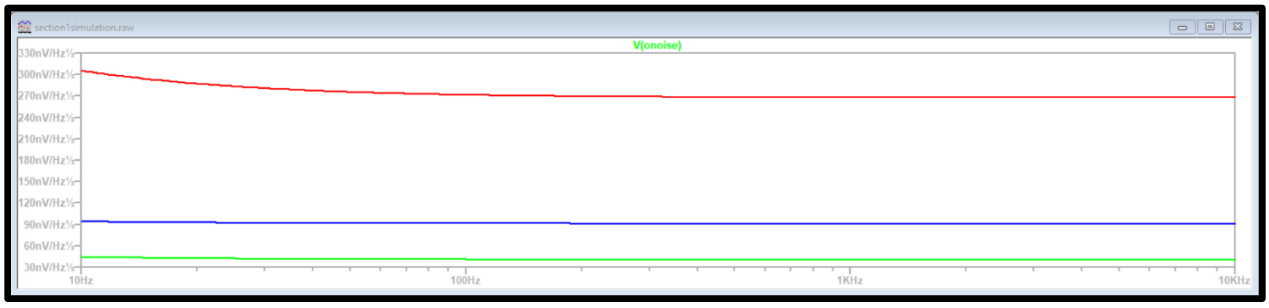

Figure 3: OP27 Noise Spectrum

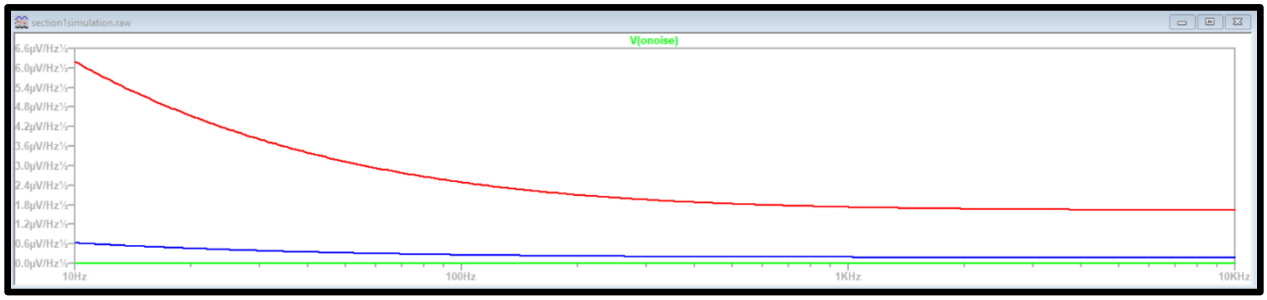

Section II/III – The following data were gathered by probing V_{out} and R_{test} during a noise simulation.

Table 1: Measured Circuit Noise Characteristics for Various Resistances

Resistance	R1 PSND $\left(\frac{\mu V}{Hz^{\frac{1}{2}}}\right)$	V_{out} PSND $\left(\frac{\mu V}{Hz^{\frac{1}{2}}}\right)$	R1 Total RMS Noise (μV)	V_{out} Total RMS Noise (μV)
100	0.269	6.002	62.19	1386.8
1k	0.852	6.12	196.66	1411.7
10k	2.694	7.099	621.89	1639.9
50k	6.024	10.417	1390.5	2405.4
100k	8.519	13.463	1966.4	3108.1
150k	10.433	15.94	2408.1	3679.5
200k	12.047	18.084	2780.4	4173.8
250k	13.468	20	3108.2	4615.8
300k	14.754	21.752	3404.5	5019.3
350k	15.936	23.375	3676.7	5393
400k	17.037	24.894	3930	5742.5
500k	19.047	27.689	4392.2	6384.9
750k	23.328	33.701	5373.3	7762.6
1M	26.935	38.825	6195.4	8929.7
3M	46.641	67.593	10517	15239
5M	60.196	88.255	13201	19347
10M	85.04	128.504	17275	26086

Note: PSND stands for Peak Spectral Noise Density

Table 2: Calculated Circuit Noise Characteristics for Various Resistances

Resistance	RMS Noise (R1/Vout)	PSND (R1/Vout)	R1 RMS^2 $(\mu V)^2$	V_{out} RMS^2 $(mV)^2$
100	0.044844246	0.044818394	3867.5961	1.923214
1k	0.139307218	0.139215686	38675.1556	1.992897
10k	0.379224343	0.379490069	386747.1721	2.689272
50k	0.578074333	0.578285495	1933490.25	5.785949
100k	0.632669477	0.632771299	3866728.96	9.660286
150k	0.654463922	0.654516939	5798945.61	13.53872
200k	0.666155542	0.666168989	7730624.16	17.42061
250k	0.673382729	0.6734	9660907.24	21.30561
300k	0.678281832	0.678282457	11590620.25	25.19337
350k	0.681754126	0.681754011	13518122.89	29.08445
400k	0.684370919	0.684381779	15444900	32.97631
500k	0.687904274	0.687890498	19291420.84	40.76695
750k	0.692203643	0.692204979	28872352.89	60.25796
1M	0.693797104	0.693754024	38382981.16	79.73954
3M	0.690137148	0.690027074	110607289	232.2271
5M	0.68232801	0.682069005	174266401	374.3064
10M	0.662232615	0.661769283	298425625	680.4794

Note: PSND stands for Peak Spectral Noise Density

Figure 4

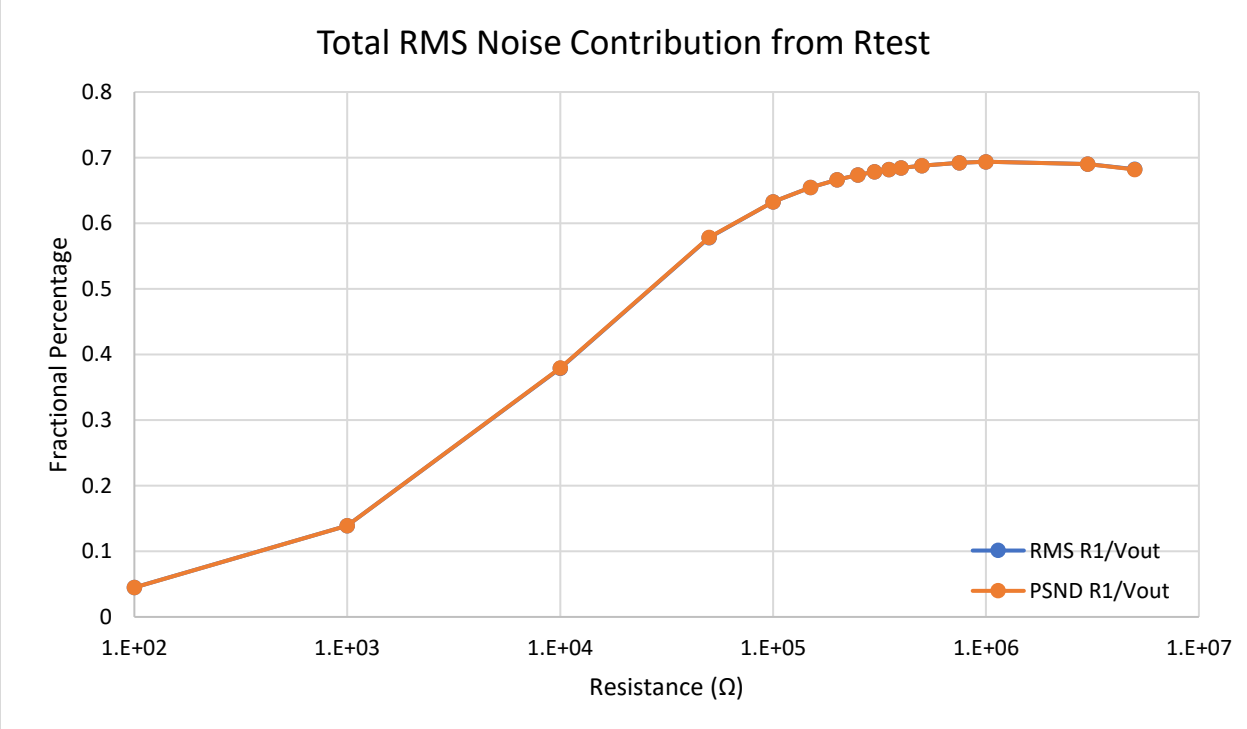

Figure 5

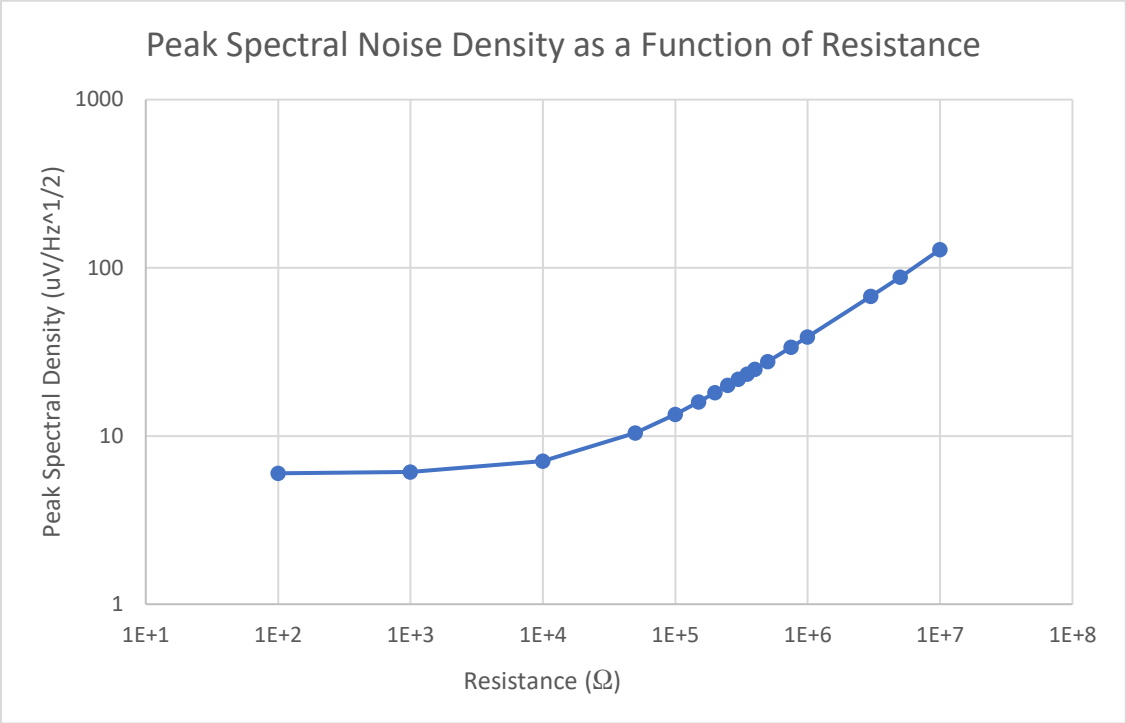

Figure 6

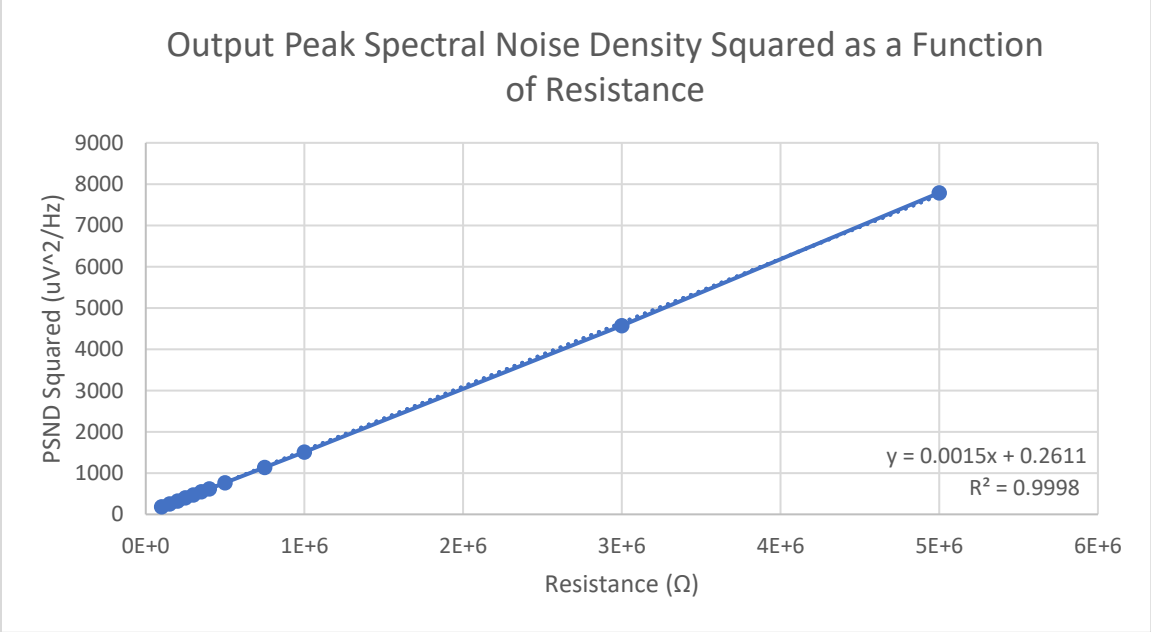

Figure 7

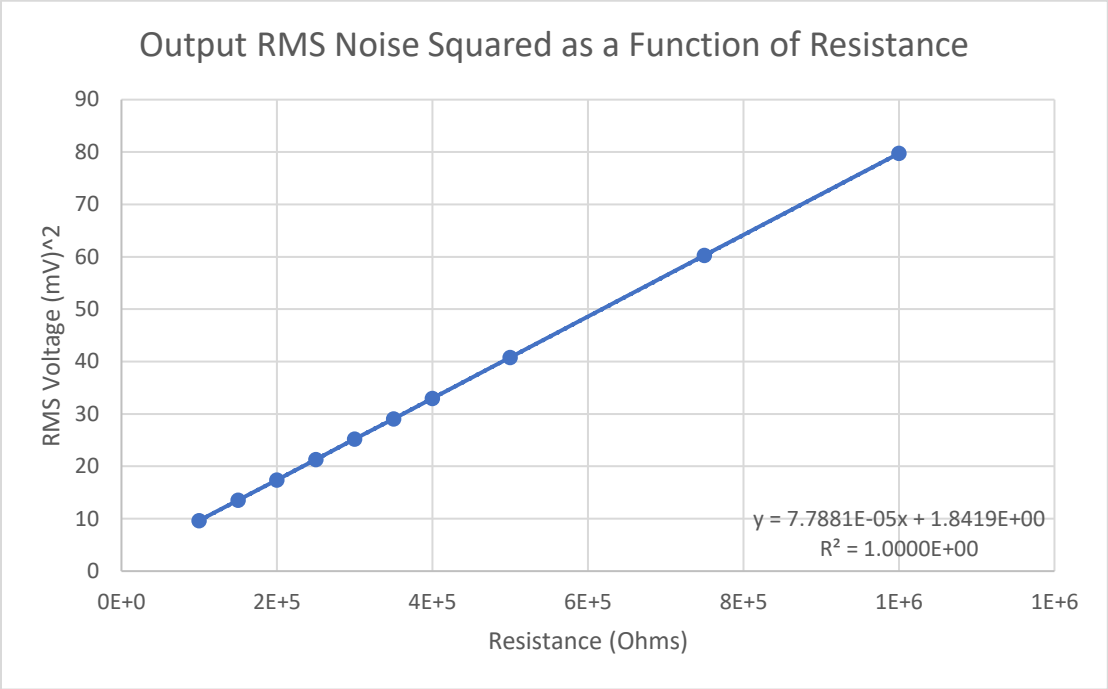

Figure 8: Gain Spectrum for Circuit Simulation

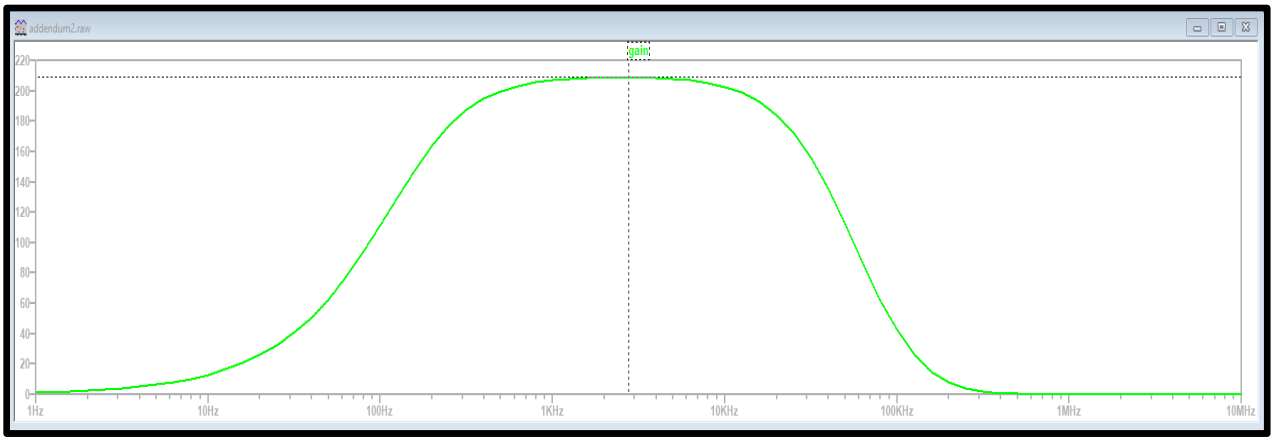

Calculating Total RMS Noise

The procedure for calculating the total RMS noise is not included in this report but can be found in the accompanying lab notebook. Using the LT1014 datasheet, it was concluded that the primary noise source with a 10kΩ resistor would be voltage noise. The gain for the op amp circuit was derived using ideal op amp rules. That gain was then multiplied by the anticipated voltage noise spectrum and the square root of the frequency bandwidth. With this technique a total RMS noise of 17.6 mV was calculated by hand. Using LTspice, the total RMS noise is 4.86 mV.

Calculating Boltzmann's Constant with Simulated Data

Starting with the equation for the signal generated by Johnson noise…

$$d\langle \bar{e}^2 \rangle = 4kRTdf$$

If this signal passes through an amplifier or other network with transfer function G, the observed output will be…

$$\langle \bar{e}^2 \rangle = 4kRT \int_0^\infty A^2 df$$

This equation is for the total noise contribution from a single resistor. However, we know our measured noise is composed of other noise sources as well. Quantitatively, looking at Figure 4, we see that in our relevant resistance range (greater than 100kΩ) the noise contribution from R_{test} to the total noise is about 69%. Therefore, we must multiply by this value.

Assuming a uniform gain profile…

$$k = \frac{0.69 \cdot \langle \bar{e}^2 \rangle}{4RTA^2\Delta f} = \frac{\langle \bar{e}^2 \rangle}{R}\frac{0.69}{4TA^2\Delta f} = \frac{(\langle \bar{e}^2 \rangle / R)}{\Delta f}\frac{0.69}{4TA^2}$$

The units for this equation equate…

$$[J \cdot K^{-1}] = \frac{[V^2/\Omega]}{[Hz]} \cdot [K^{-1}] = \frac{[J/s]}{[s^{-1}]} \cdot [K^{-1}] = [J \cdot K^{-1}]$$

The term $\frac{(\langle \bar{e}^2 \rangle / R)}{\Delta f}$ can be found from the slope of Figure 6. We have the other values as well:

- $T = 300°K$ – The default value or simulations in LTspice.
- $A = 242$ – The value for A is derived using ideal op amp rules. The details of the calculation are not paramount to this report but can be found in the accompanying lab notebook.

Now, substituting all values…

$$k = \frac{(\langle \bar{e}^2 \rangle / R)}{\Delta f}\frac{0.69}{4TA^2} = (0.0015 \cdot 10^{-12}[J]) \cdot (\frac{0.69}{4 \cdot 300 \cdot 242^2}[K^{-1}])$$

$$k = 1.472 \cdot 10^{-23}\, JK^{-1}$$

Similarly, we can calculate using the RMS data. If we use the slope of Figure 7 we have $\frac{RMS^2}{R}$.

$$k = \frac{\langle \bar{e}^2 \rangle}{4RTA^2\Delta f} = \frac{\langle \bar{e}^2 \rangle}{R}\frac{0.69}{4TA^2\Delta f} = \frac{RMS^2}{R}\frac{0.69}{4TA^2\Delta f}$$

From the gain spectrum in Figure 8 we see that most of the noise will come from between 100Hz and 100kHz. Approximating Δf = 100kHz and substituting other quantities we get…

$$k = \frac{RMS^2}{R}\frac{0.69}{4TA^2\Delta f} = \frac{(7.881 \cdot 10^{-11})}{4 \cdot 300 \cdot 242^2 \cdot 100 \cdot 10^3}$$

$$k = 0.773 \cdot 10^{-23}\, JK^{-1}$$

Section IV – The following data were gathered by probing V_{out} of the physical circuit.

Table 3: Output RMS Voltage (mV)

Resistance	1	2	3	4	5	6	7	8	AVG	AVG^2 (mV^2)
2MΩ	8.31	8.16	9.26	7.99	7.87	8.06	7.88	8.06	8.19875	67.2195016
1MΩ	6.35	6.23	7.3	6.29	6.5	6.63	6.32	7.05	6.58375	43.3457641
470kΩ	4.8	6.34	4.97	4.98	6.55	4.95	5.12	4.73	5.305	28.143025
100kΩ	3.44	3.52	3.28	3.04	3.7	4.33	4.16	3.17	3.58	12.8164
47kΩ	2.49	2.6	3.12	2.57	2.69	2.67	3.59	3.3	2.87875	8.28720156
18kΩ	2.92	2.87	2.63	2.68	2.48	2.91	2.42	2.95	2.7325	7.46655625
2.2kΩ	2.71	2.17	2.76	2.59	2.32	2.44	2.46	2.11	2.445	5.978025
100Ω	1.7	2.11	1.69	1.88	1.72	1.88	2.07	1.66	1.83875	3.38100156

Figure 9

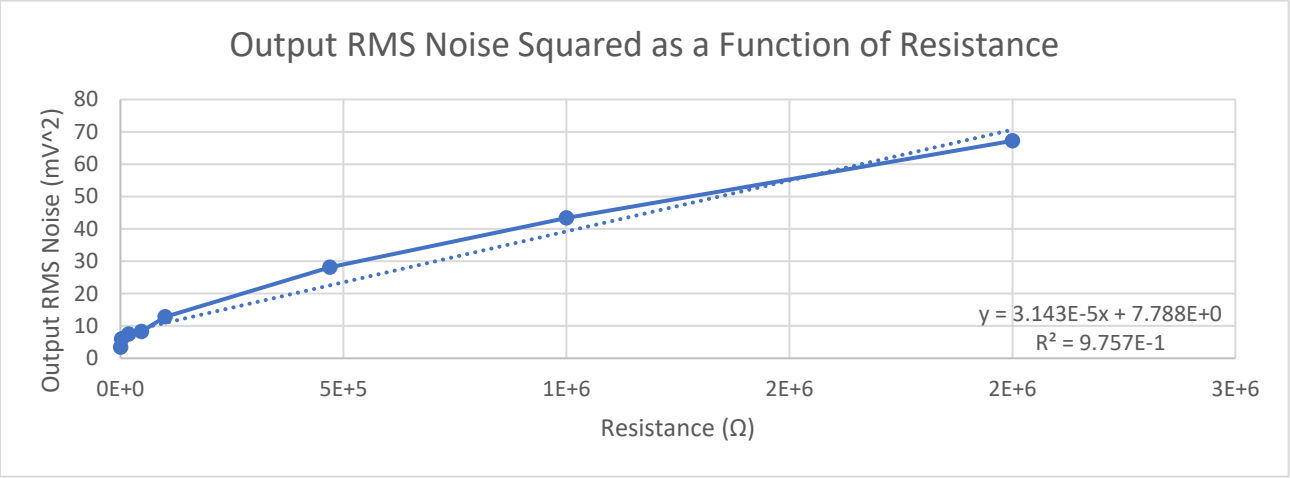

Figure 10

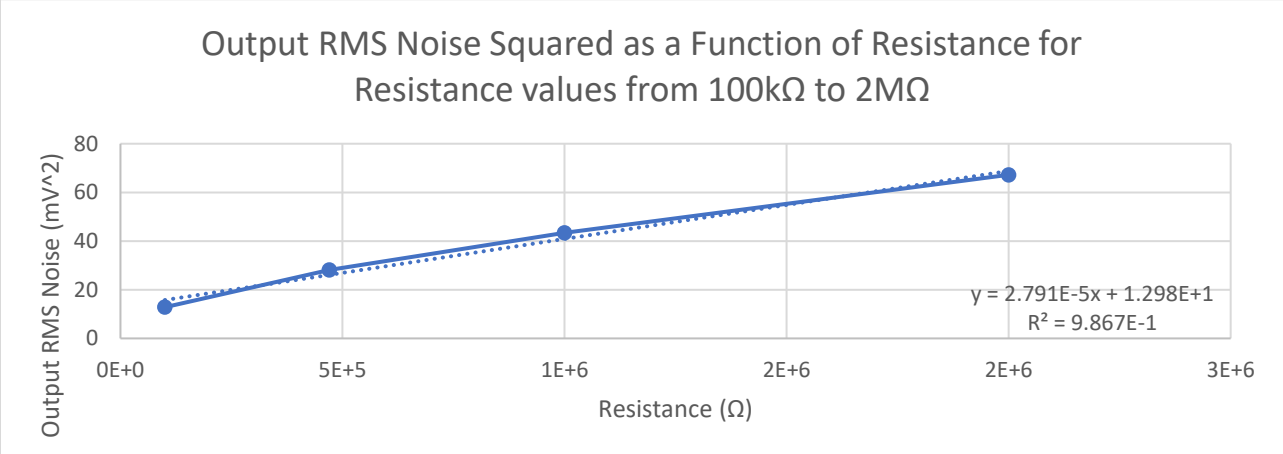

Calculating Boltzmann's Constant with Real Data

Again, we start with the equation for the signal generated by Johnson noise…

$$d\langle \bar{e}^2 \rangle = 4kRTdf$$

And come to the same equations relating Boltzmann's constant to the ratio between Peak Spectral Noise Density or RMS noise squared and resistance.

$$k = \frac{(\langle \bar{e}^2 \rangle / R)}{\Delta f}\frac{0.69}{4TA^2} = \frac{RMS^2}{R}\frac{0.69}{4TA^2\Delta f}$$

However, given the MyDAQ equipment used to acquire physical data, we do not have measurements for the PSND. There are two key distinctions in our physical calculation as opposed to the simulated calculations.

Firstly, the frequency range is much smaller than in the simulation. The MyDAQ has a peak frequency of 20kHz, therefore the frequency bandwidth is only 20kHz.

Secondly, from Section I, we know the main contributor to noise at low resistances is not the Johnson noise of the resistors; Johnson noise does not take precedence until higher resistances. In Figure 9 we clearly see a nonlinear nature in the lower resistance regime. However, at higher resistances the regression linearizes. The exact regime in which Johnson noise dominates can be seen from Figure 4. The data plateau around 100kΩ. This is interpreted in Section II of the discussion. We will use its result now by restricting the domain of our measurements to be greater or equal than 100kΩ. The results are seen in Figure 10, from which we will pull our measurement for the slope to be used in calculating Boltzmann's constant below.

Substituting values…

$$k = \frac{RMS^2}{R}\frac{0.69}{4TA^2\Delta f} = \frac{2.791 \cdot 0.69 \cdot 10^{-5} \cdot 10^{-6}}{4 \cdot 300 \cdot 242^2 \cdot 20 \cdot 10^3} = 1.370 \cdot 10^{-23} JK^{-1}$$

This result is remarkably close to the actual value for Boltzmann's constant! It most likely pushes the limits of the accuracy of our experimental setup.

DISCUSSION

The following sections will discuss the data collected in each corresponding Results subsection.

Section I – The data presented shows the noise spectrum for three different op amps.

From an initial glance, it is evident that the AD795 and the LT1014 behave much more similarly than the OP27. This behavior is exaggerated when a 1 MΩ test resistor is used. Again, referencing the Analog Devices' MT-047 Tutorial, we know that current noise flowing through a test resistor is typically dominant at test resistance values. For this reason alone, we can suspect that the AD795 and LT1014 may be low current noise op amps, whereas the OP27 is not. This would therefore make the OP27 a poor candidate for measuring the Johnson noise in the test resistor, since there would be a small signal to noise ratio (if we consider Johnson noise as the signal and other noise sources as noise). Therefore, we will narrow our analysis to the AD795 and LT1014.

Again, looking at the 1MΩ curve, we see that outside the scope of flicker noise both the AD795 and the LT1014 have frequency noise spectrums of approximately $270\ nV/\sqrt{Hz}$. One thing of note is that the LT1014 contains flicker noise corner around 50Hz whereas it is difficult to make out if the AD795 has a flicker noise corner at all. This would make the AD795 marginally better in high input impedance, low frequency applications.

At low resistances, we know that the Johnson noise produced by the test resistor is low and that the current noise through the test resistor will also be low. For this reason, low test resistance values are in the regime where op amp voltage noise is dominant. Comparing our two op amps we see two different shapes for our 100Ω curves. The LT1014 has flat spectral density whereas the AD795 has a significant increase at lower frequencies, again corresponding to flicker noise but with the other op amp. Despite having more prominent flicker noise, by approximately 50Hz, the AD795 has a lower noise output than the LT104.

It is difficult to draw information from our medium input resistance range, 100kΩ. At this input impedance either Johnson noise or current noise could dominate. Further, despite differences in the flicker noise regime again, both op amps before approximately the same above 100Hz.

In conclusion, these op amps are quite comparable. They have some clear distinctions regarding flicker noise. The AD795 appears to have greater voltage flicker noise whereas the LT1014 appears to have greater current flicker noise. Beyond this, their current noise seems to be very close. However, the AD795 appears to be a clear winner with regards to voltage noise if the domain is restricted to above approximately 50Hz. Both the AD795 and the LT1014 appear to have significantly lower input current noise than the OP27.

By looking at their respective datasheets, our analysis is confirmed. Some key clarifications are that at 10Hz the input current noise is 70 $fA/\sqrt{Hz}$ for the LT1014 but only 13 $fA/\sqrt{Hz}$ for the AD795. This difference, however, is quite small when compared with the 1.7 $pA/\sqrt{Hz}$ for the OP27, therefore their similar behavior is understandable. On the contrary, although voltage noise is not much concern for this lab, the OP27 has considerably lower voltage noise than the other two op amps.

Section II – Our hand calculation for the total RMS noise is 17.6 mV whereas LTspice calculates 4.86 mV. While our hand calculation is quite a bit higher than expected, it is the correct order of magnitude and therefore we have a decent analysis. Further, it is well within the factor of five threshold requested by the lab procedure. It can be reasonably suspected that the difference between the values is a result of the ideal op amp approximation. In reality we do not have infinite gain. Further, the gain profile for real op amps does not have a flat frequency spectrum. Figure 8 contains the gain spectrum for our circuit. It peaks at 210 and contains a lower and upper corner at about 100Hz and 100kHz. For these reasons, we should be happy with the accuracy of our approximation.

Section III – In this section of the lab we collected and manipulated a lot of data. Ultimately, we calculated Boltzmann's constant two different, but related, ways. Part of this discussion is intrinsically part of the calculations made in the corresponding Results section.

Starting with Figure 4, we can analyze the contribution of noise from R_{test} to the total output noise. This measurement is a courtesy of LTspice; it is not possible to measure the noise across a single resistor with our physical experimental setup. From our data, we see that the noise contribution from R_{test} rises until

around 100kΩ. At this value, the noise contribution levels at about 70%. The data above 100kΩ appear to be concave down and so we anticipate that the noise contribution would again drop down, but that is beyond the measured resistances for this lab. Regardless, we have a bandwidth from approximately 100kΩ to 5MΩ where the noise contribution from R_{test} to the total noise is roughly constant. We can interpret this as being the bandwidth in which Johnson noise dominates our total circuit noise.

Moving on, we also measured the peak spectral noise density (PSND) of our noise as a function of resistance, this can be found in Figure 5. The PSND is approximately constant at lower frequencies but has a corner frequency around 50kΩ. At this point the data become linear in a log-log scale. Considering we know that Johnson noise dominates from 100k to 5MΩ, we can restrict our graph to that bandwidth as done in Figure 6. With this restricted domain we can fit a function to our graph with incredible agreement. As explained in the calculations the slope of these restricted data is what allows us to calculate Boltzmann's constant. An advantage of this calculation is that there is no dependency of the frequency spectrum being measured. In fact, we only need a single point for a reasonable calculation. We use the slope to further increase the accuracy of our calculation. Using this method, we arrived at a final answer for Boltzmann's constant to be $1.472 \cdot 10^{-23} J/K$. Knowing that Boltzmann's constant is actually $1.381 \cdot 10^{-23} J/K$ we get an error of…

$$Percent\ Difference = \left|\frac{observed - expected}{expected}\right|$$

$$\%dif = \left|\frac{1.381 - 1.472}{1.381}\right| = 6.6\%$$

… this is in very good agreement with the true value.

There is however, still some error. A very plausible source of error could again be the gain factor. In calculating Boltzmann's constant, this gain factor appears in an integral over frequency. We assume that we have a uniform gain profile to simplify our calculations. This simplification, however, is very much not true as is again evident by Figure 8. Our gain spectrums frequency dependence is probably accentuated further by the act of integration.

In addition to calculating Boltzmann's constant using the PSND, we also calculated it used the total output RMS Noise squared. We can see the regression for the RMS noise squared as a function of resistance in Figure 7. We used the same domain as before except we restricted the upper limit to 1MΩ so that we could better fit a linear regression to the data. Following our calculations in the Results section, we arrived at a value for Boltzmann's constant of $0.773 \cdot 10^{-23} J/K$. The corresponding error is…

$$\%dif = \left|\frac{1.381 - 0.773}{1.381}\right| = 44.0\%$$

… this error is quite large, evidently this calculation is less accurate than using the PSND.

We can suspect two main sources of error. When calculating using the RMS noise, we would expect the same error regarding the gain factor as when using the PSND. Further, we now have additional uncertainty/error associated with including a frequency bandwidth. For our calculation we used 100kHz because that is the apparent range of high gain, seen in Figure 8. This choice of 100kHz, although justified, is by no means precise. Perhaps we should have used a frequency bandwidth of 200kHz, in which case our calculation would be much better. As such, our uncertainty in this calculation is high.

Regardless, we came within the correct order of magnitude for both calculations. This is impressive considering some of the approximations made. Potentially one of the most impactful ways to improve this calculation would be fitting a function to the gain profile of the circuit and using that in our calculations.

Section IV – The final section of this lab attempted to repeat the procedure of the previous section. However, rather than using simulations we use a physical circuit and real data. Using actual measurements of course gave rise to many problems.

For starters, when trying to measure a particular source of noise you are inevitably burdened with various other sources of noise. We have already discussed the necessary inclusion of a shield around our circuit. Shielding helps a lot but is not perfect. The MyDAQ dynamic signal analyzer is particularly helpful in determining whether additional noise sources are present. The noise spectrum of Johnson noise is flat. Therefore, if you see any peaks apart from the expected peak associated with flicker noise, then you know your circuit is being contaminated. For instance, if a cell phone is held to near to the circuit, even with shielding, you will see multiple peaks in the frequency spectrum at integer multiples of 10kHz. A particular problem when measuring data was the noise generated by the computer used to measure that data, as the wire connecting the MyDAQ to a laptop is not very long. A curious problem persists when you hold one hand near the circuit and one near your computer to collect data. A similar noise spectrum to when them computer is held close to the circuit is seen. It is suspected that your body acts as a conductor for the electromagnetic waves to propagate from the computer to the circuit. The necessary solution to this problem is to first make measurements and then record data, we can not do the two simultaneously.

Once these hurdles are overcome, the data produced can be quite nice. As with the simulations, we again had a nonlinear relationship between total output RMS noise squared and resistance if we look at a very broad frequency spectrum, as seen in Figure 9. However, again restricting ourselves to the relevant resistance domain where Johnson noise is dominant, Figure 10, we see a relatively linear regression.

As we did for Section III, we again calculated Boltzmann's constant using our RMS data. The exact calculation can be found in the Results section. We arrive at a value of $1.370 \cdot 10^{-23} J/K$. Calculating the error…

$$\%dif = \left|\frac{1.381 - 1.370}{1.381}\right| = 0.80\%$$

This is incredibly low error considering the magnitude of Boltzmann's constant. So close that suspicion arises.

Further, having our real measurements be more accurate than our simulations is suspicious by itself. At first glance, as with the simulations, we would expect a potential source of error to be the gain profile of our circuit. However, unlike our simulations we have a small and definitive frequency spectrum. The MyDAQ is limited to making measurements below 20kHz. In this range, the gain is much more constant. We still have a very low gain from 0Hz to approximately 300Hz. But, in the much more massive 300Hz to 20kHz range the gain is close to constant (again, Figure 8). Therefore, both our error regarding the gain profile and our error regarding the division by our frequency spectrum should be much less than in our simulations. Despite this optimism, our measurement techniques and calculations would have to be further reviewed before we can conclude the legitimacy of our results.

CONCLUSION

This lab studied the implications of noise in electronics circuits. Through this lab we developed an understanding of the current noise and voltage noise produced by the AD795, LT1017, and OP27. We then went on to determine the regime in which Johnson noise dominates a particular circuit. With that information we examined the total RMS output noise and peak spectral noise density of our circuit in both a simulated and physical format. Finally, with our data we calculated Boltzmann's constant to good accuracy in our simulations and incredible accuracy in our physical measurements.

RESOURCES

Noise Analysis in Operational Amplifier Circuits Application Report, SLVA043B, Texas Instruments, 2007. [Online]. Available: https://www.ti.com/lit/an/slva043b/slva043b.pdf?ts=1615054681509

MT-047 Tutorial, Analog Devices, 2009. [Online]. Available: https://www.analog.com/media/en/training-seminars/tutorials/MT-047.pdf

Low Power, Low Noise Precision FET Op Amp, Rev. D, Analog Devices, 2019. [Online]. Available: https://www.analog.com/media/en/technical-documentation/data-sheets/ad795.pdf

LT1014, LT1014A, LT1014D Quad Precision Operational Amplifiers, SLOS039D, Texas Instruments, 2009. [Online]. Available: https://www.ti.com/lit/ds/symlink/lt1014.pdf?ts=1615057938415&ref_url=https%253A%252F%252Fwww.ti.com%252Fproduct%252FLT1014%253Futm_source%253Dgoogle%2526utm_medium%253Dcpc%2526utm_campaign%253Dasc-null-null-GPN_EN-cpc-pf-google-wwe%2526utm_content%253DLT1014%2526ds_k%253DLT1014%2BDatasheet%2526DCM%253Dyes%2526gclid%253DCj0KCQiA7YyCBhD_ARIsALkj54rKkiuyIhRqeMTrj-nIOXNlQX3HQ0Us3HK5W1V3yTIH3nBcxd1uKhwaAodlEALw_wcB%2526gclsrc%253Daw.ds

Low Noise, Precision Operational Amplifier, 0P27, Analog Devices, 2015. [Online]. Available: https://www.analog.com/media/en/technical-documentation/data-sheets/OP27.pdf